

---

## **Non-diagonal transport phenomena in deep disposal facilities: contribution of osmotic processes to the interpretation of the far-field water pressure in the Tournemire argillite**

*Matray Jean-Michel\*, Tremosa Joachim\*, \*\**

\*IRSN / BP 17 F 92262 Fontenay-aux Roses cedex (France)

\*\* present adress BRGM, BP36009, 45060 Orléans cedex 2 (France)

---

### **Abstract:**

This study aims at identifying and quantifying the contribution of each mechanism that may contribute to the excess hydraulic heads measured in the Toarcian/Domerian clay rock at Tournemire. Such excess heads are very close to those measured by Andrain in the Callovian-Oxfordian argillite at the Bure URL and considered as a possible host rock for a HL-ILLL repository. A special focus is made on transport processes such as advection, chemo-osmosis and thermo-osmosis, respectively responsible for a fluid flow under gradients of pressure, concentration and temperature. The quantification of their relative contribution has required to acquire their force gradients and their related parameters. A 1D modeling approach based on the application of continuity equation at steady state is proposed. A satisfactory reproduction of the measured excess hydraulic head is achieved by coupling chemo-thermo-osmotic flows to advection. Those simulations also allowed comparing the characteristic times for diffusion to advection including non-diagonal osmotic flows. Results suggest that diffusion still remains the dominant transport phenomenon for solutes and therefore for RN at the formation scale. However, the introduction of thermo-osmotic flow in the calculations leads to an increase of the specific discharge and to reverse the water movements which become directed upward.

## 1 BACKGROUND

Excess-head pressures are frequently observed in aquitards such as shales and argillites compared to the theoretical hydrostatic profile deduced from hydraulic heads measured in their surrounding non-argillaceous aquifers. This is the case for the Callovo-Oxfordian argillite studied by Andra as a potential host rock for the repository of High Level and Intermediate Level Long-Lived radioactive wastes. This formation is known to develop an excess-head of about 50m in equivalent water level measured at the centre of the 150m-thick Callovo-Oxfordian (COx) formation and located at a mean depth of about 475m/bslin the vicinity of their deep Underground Research Laboratory (URL), located in the East of France[1]. An excess-head of about 30m was also identified in the centre of the 250m-thick Toarcian/Domerian over-consolidated clayrock at the IRSN's URL in Tournemire (Figure 1), located in the South of France[2],[3]. Data reported in this figure are not affected by the tunnel or drifts influence[2] which tend to deplete the pore pressure and are therefore representative of the far-field water-pressure conditions.

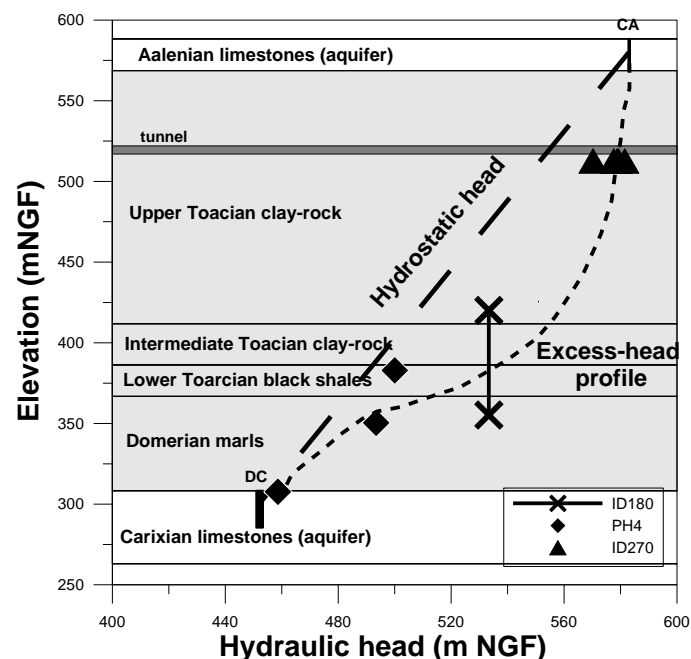


Figure 1: Hydraulic head profile at the Tournemire URL across the Toarcian/Domerian clayrock representative of far-field conditions with respect to the tunnel.

Several researchers [4], [5] agreed that excess-heads may result from one or more of the following mechanisms related to: i) mechanical stresses such as compaction disequilibrium of the argillaceous formation or skeleton deformation of the sediment under tectonic stress, ii) diagenetic stresses during mineralogical transformation or neoformation, iii) changes in hydrodynamic boundary conditions, iv) hydromechanical processes including the viscoplastic behaviour of clays, and v) transport processes including non-diagonal one such as osmotic processes.

Andra first proposed that the chemo-osmotic phenomenon alone was able to explain the excess head [1] at their Bure site but decided to conduct a new study next to the assessment by IRSN that the contribution of other processes was likely [6]. The goal of this study was to assess the relative contribution of osmotic processes to the measured overpressures. It also aimed at verifying whether the coupling of transport processes involving gradients of hydraulic and chemical potentials on the water flux alone could account for such an excess head. The conclusions based on in situ and lab experiments and also on a numerical approach of transport processes at steady state were unambiguous. The chemical osmotic effect estimated in the Callovo-Oxfordian coupled to advection could only explain 10m out of the 20-50m of the measured excess heads [7].

During this study, the lab tests performed on remolded COx samples for determining their osmotic efficiency also showed the role of temperature on the pressure signal suggesting the participation of another transport process: Thermo-osmosis. This process was poorly characterized so that no satisfactory expression to calculate its contribution was available nor thermo-osmotic experiments performed on natural shales, so far.

As there was no satisfactory model to explain the excess-head at the Bure site, IRSN decided to conduct its own research programme at the Tournemire URL with the goal of identifying and quantifying the contribution of each cause to the measured excess-head. The purpose of this study was to determine whether or not the osmotic phenomena may be considered as responsible for such pressure profile at the Tournemire site.

First, a special attention is paid in section 2 to the definitions of individual flows in compacted clay rocks. This includes the Darcy's flow and osmotic flows, i.e. the coupled fluid fluxes induced by chemical concentration, temperature and electrical gradients, in natural compacted clay rocks. Section 3 deals with the modelling of the hydraulic head profile across the Tournemire clay rock, which includes the determination of force gradients and of coupled flow parameters profiles through the clay rock. The modelling of individual and coupled fluid flows at steady state and comparison to the measured one, and to finish the contribution of coupled advective flows to the solute transport is assessed. At last the role of other possible processes such as transient hydromechanical to the excess head are also discussed.

Results presented in this paper were mostly obtained in the PhD of J. Tremosa [3] who performed its thesis work at IRSN between 2008 and 2010.

## 2 COUPLED FLUID FLOWS IN CLAY ROCKS

### 2.1 Theory

Coupled-flows in clay rocks originate from the electrochemical interactions occurring at the pore scale between the charged surface of clay minerals and the water and electrolytes. Due to isomorphic substitutions of cations by others having a lower valence, in tetrahedral and octahedral layers, clay minerals present a surface charge, negative at natural pH, which induces a non-uniform distribution of cations, anions and water molecules. The solute distribution in the pore space results from the combination of the attraction by the charged surface and their diffusion towards the pore center, where solute concentration is lower [8]. The ion distribution and the electrical potential can be described using double layer or triple layer electrical models [8].

The Onsager's matrix (Table 1) summarizes the flows which can develop under the different potential gradients [9], [10]. This includes fluxes related to their natural gradient, the diagonal flows, as well as the fluxes occurring under the other potential gradients, i.e. the non-diagonal fluxes.

Table 1 also shows that the surrounding transport processes accounting for water flow are limited to Darcy flow and osmotic processes.

Flux	Gradients			
	Hydraulic head	Electrical	Chemical concentration	Temperature
Fluid	Darcy	Electro-osmosis	Chemical osmosis	Thermo-osmosis
Current	Electrofiltration	Ohm	Membrane potential	Thermo-electricity
Ion	Ultrafiltration	Electrophoresis	Fick	Soret effect
Heat	Thermal filtration	Peltier effect	Dufour effect	Fourier

Table 1: Onsager matrix with coupled-flows terminology

Coupling coefficients relating a flux to a driving force can be characterized through the principles of the irreversible thermodynamics, based on the notion of entropy, and assumes a linear relation between the flows  $J_i$  and the gradients  $X_i$ , as follows [11]:

$$J_i = \sum_{j=1}^n L_{ij} X_j \quad \text{Eq. 1}$$

where the subscripts  $i$  and  $j$  correspond to the various kinds of flows and gradients, respectively and  $L_{ij}$  are the phenomenological coefficients. The coefficients of the coupled flow matrix can then be obtained during experiments, i.e. measuring the flow associated to a force gradient.

When chemical osmosis, thermo-osmosis and electro-osmosis are considered together with the Darcy's flow, the fluid flow equation is extended and writes:

$$q = -\frac{k}{\eta} (\nabla P + \rho_f g \nabla z) + \frac{k_o}{\eta} \nabla \Pi - \frac{k_T}{\eta} \nabla T + \beta \nabla \varphi \quad \text{Eq. 2}$$

where  $q$  is the pore fluid specific discharge ( $\text{m s}^{-1}$ ),  $\eta$  the dynamic viscosity ( $\text{Pa s}$ ),  $\rho_f$  the fluid density ( $\text{kg m}^{-3}$ ),  $g$  is the acceleration due to gravity ( $\text{m s}^{-2}$ ),  $k$ ,  $k_o$  and  $k_T$  denote the Intrinsic permeability ( $\text{m}^2$ ), the chemo-Osmotic permeability ( $\text{m}^2$ ) and the Thermo-osmotic permeability ( $\text{m}^2 \text{s}^{-1} \text{K}^{-1}$ ) respectively and  $\beta$  is the electro-osmosis coefficient ( $\text{m}^2 \text{s}^{-1} \text{V}^{-1}$ ).  $\nabla P$ ,  $\nabla \Pi$ ,  $\nabla T$ ,  $\nabla \varphi$  represent the gradients of the pressure (Pa), osmotic pressure (Pa), temperature ( $^\circ\text{K}$ ), and current (A). The last three terms in Eq. 2 can be considered as the non-diagonal transport phenomena and represent the osmotic contribution to the fluid flow.

## 2.2 Darcy flow

The contribution of the Darcy flow to the pore specific discharge may be deduced from Eq. 2:

$$q = -\frac{k}{\eta} (\nabla P + \rho_f g \nabla z) \quad \text{Eq. 3}$$

For a porous medium with a plane, parallel pore geometry, intrinsic permeability  $k$  can be obtained using a Poiseuille law:

$$k = b^2/3F \quad \text{Eq. 4}$$

where  $F$ , the formation factor accounting for the tortuosity of the porous media, is defined as  $F = \omega^{-m}$  with  $\omega$  the porosity and  $m$  the cementation factor [13] which is rock dependent and must be defined for each case study. And  $b$  is the half-pore size (m) defined as:

$$b = \frac{\omega}{\rho_s A_s (1 - \omega)} \quad \text{Eq. 5}$$

with  $\omega$  the total porosity,  $\rho_s$  is the grain density ( $\text{g m}^{-3}$ ) and  $A_s$  is the specific surface area ( $\text{m}^2 \text{g}^{-1}$ ). It is worth noting that anion exclusion expression is applicable for both symmetric and nonsymmetric solutions [10].

The fluid density  $\rho_f$  ( $\text{kg m}^{-3}$ ) can be calculated from the Unesco equation of state which depends on salinity, temperature and pressure [14]. The dynamic viscosity of water ( $\eta$  in Pa·s) can be determined using the relation given in reference [15] as a function of temperature:

$$\frac{1}{\eta} = (5.38 + 3.8A - 0.26A^3) \times 10^3 \quad \text{Eq. 6}$$

where  $A = \frac{(T-150)}{100}$  with  $T$ , the temperature, expressed in °C.

## 2.3 Osmotic flows

### 2.3.1 Chemical-osmosis

Chemical osmosis is the fluid flow across a material exhibiting a membrane behaviour induced by a difference of chemical potential. A membrane is a material which limits the transport of ionic species but not the movement of neutral species such as water. Differences in concentration between two reservoirs induce a difference in osmotic pressure such as:

$$\Pi = -\frac{RT}{\Omega_w} \ln a_w \quad \text{Eq. 7}$$

where  $\Pi$  is the osmotic pressure (Pa),  $R$  is the gas constant ( $8.32 \times 10^{-3} \text{ m}^3 \text{Pa K}^{-1} \text{mol}^{-1}$ ),  $T$  is the temperature (K),  $\Omega_w$  is the molar volume of water ( $\text{L mol}^{-1}$ ) and  $a_w$  is the water activity which depends on the aqueous concentration in the solution.

The osmotic efficiency coefficient of a clayrock writes  $\varepsilon$  and ranges between 0 for non-membrane behavior and 1 for perfect membrane behavior, where solute flux is totally inhibited. The pore fluid specific discharge ( $\text{m s}^{-1}$ ) of the chemical-osmosis flow deduced from Eq. 2 thus writes:

$$q = -\frac{k}{\eta} (\nabla P + \rho_f g \nabla z) + \varepsilon \frac{k}{\eta} \nabla \Pi \quad \text{Eq. 8}$$

The  $\varepsilon$  coefficient can be determined experimentally (see [3] and references therein). The osmotic efficiency can also be computed in a predictive sense using theoretical models that consider the electrical interactions between the solution and the charged surface together with the petrophysical properties of the porous media [13], [16], [17], [18]. Predictive models allow to have osmotic efficiency coefficients for a wide range of salinity and pore size conditions and more easily than from experiments. Experiments are however essential for model calibration and to demonstrate that the studied clayrock develops a membrane behaviour. The chemo-osmotic efficiency is obtained from the Navier-Stokes equation integrating the chemical force [11]:

$$\varepsilon = \frac{\int_0^b \left(1 - \frac{\bar{C} - (x)}{C_f}\right) (2bx - x^2) dx}{\frac{2b^3}{3}} \quad \text{Eq. 9}$$

where  $\bar{C} - (x)$  is the anion concentration at a distance  $x$  from the clay surface,  $C_f$  is the anion concentration in the equilibrium solution, and  $2b$  the pore size (m) defined for a plane, parallel pore geometry. However, overpressures predicted by this combined model (Eq. 8+Eq. 9) are systematically higher than the observed one [19]. This was attributed by [20] to two natural causes: the effect of the complex composition of natural waters, including both monovalent and divalent cations, on the osmotic efficiency and the resulting abnormal pressures, and the presence of steady state rather than transient-state salinity distributions.

For this purpose, an electrical triple-layer model (TLM) accounting for multi-ionic solutions was developed and used to calculate the osmotic efficiency at different proportions of monovalent and divalent cations (see Appendix A in [20]). The evolution of the chemo-osmotic efficiency coefficient calculated with the TLM as a function of the calcium index (Cal) is reported in Figure 2.

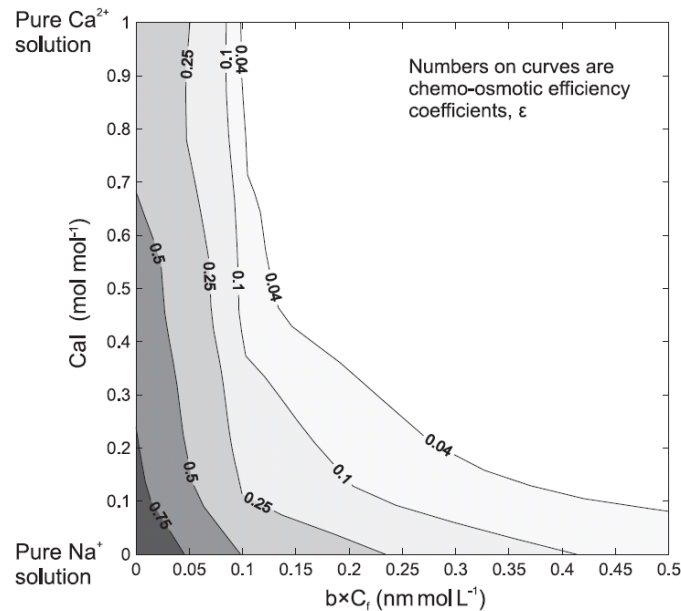


Figure 2: Evolution of chemo-osmotic efficiency coefficient calculated with the TLM as a function of the calcium index (Cal),  $2x\text{Ca}^{2+}/(\text{Na}^{+}+\text{Ca}^{2+})$ , and  $b \times C_i$  [20].

Figure 2 illustrates that  $\varepsilon$  decreases when the salinity ( $C_f$ ) and/or the pore size ( $b$ ) increase, and also when the counterions are  $\text{Ca}^{2+}$  versus  $\text{Na}^{+}$ . At large pore size and for high bulk concentration, the electrical double layer collapses resulting in weak anionic exclusion.

### 2.3.2 Thermo-osmosis

Thermo-osmosis is a fluid flow driven by a temperature gradient. The macroscopic transport coefficient for the thermo-osmotic permeability  $k_T$  was proposed from a microscopic analysis as  $k_T = \frac{k\Delta H}{T}$  [21] yielding to the following fluid specific discharge equation:

$$q = -\frac{k}{\eta} (\nabla P + \rho_f g \nabla z) - \frac{k \Delta H}{\eta T} \nabla T \quad \text{Eq. 10}$$

where  $q$  is the pore fluid specific discharge ( $\text{ms}^{-1}$ ),  $T$  is the temperature (K) and  $\Delta H$  is the macroscopic volume-averaged excess specific enthalpy due to fluid–solid interactions ( $\text{J m}^{-3}$ ). This difference  $\Delta H$  is associated with an alteration of the hydrogen bond (HB) network of the water molecules and thus of the intermolecular bond energy due to fluid–solid interactions. A fully predictive theoretical expressions for  $k_T$  was developed by directly formalizing the enthalpy change  $\Delta H$  due to hydrogen bonding modifications at the macro-scale [22].

### 2.3.3 Electro-osmosis

Electro-osmosis describes the flow of fluid due to an electrical potential gradient. However, in natural systems, the macroscopic current density is considered nil [11] and allows writing the electrical potential gradient as a function of the other gradients and coupling coefficients. This leads to an implicit integration of electro-osmosis in the flow coupling coefficients related to the pressure, chemical potential and temperature gradients [11] and which therefore turn as apparent coefficients.

## 3 MODELLING THE CLAYROCK POREWATER HEADS

### 3.1 Modelling concept

The aim of these calculations is to establish the effect of the osmotic flow on the head profile in the clayrock (Figure 1). The individual and coupled effects of chemical osmosis and thermo-osmosis were studied assuming that electro-osmosis flow is negligible. Calculations were made in 1D, along the  $z$ -axis, in the Toarcian/Domerian layers using the pressure, temperature conditions determined for the Carixian and Aalenian aquifers as boundary conditions and the concentration profile determined for the clayrock. These calculations allowed obtaining a pressure profile across the argillaceous formation and, after transformation as a hydraulic head, comparing it to the hydraulic head monitored in the formation and reported in Figure 1. In the present calculations, a pressure build-up was calculated for a given profile of concentration and temperature, considering that at a given time, the modeled system is in pseudo-equilibrium, so that the variations of pressure with time can be assumed nil. This simplification can be made because of the very low hydraulic diffusivity and diffusion coefficient of the Tournemire clayrock [20]. The election of steady-state conditions for the calculations presents the interest to avoid performing a reconstruction of the basin evolution including the flows and transfers in the clayrock, required for transient-state calculations. An assessment of such hypothesis is discussed in section 3.4.4.

The pressure field in the formation is finally calculated by solving the pressure - diffusion equation including osmotic coupled flows at steady-state:

$$\frac{\partial}{\partial z} \left( \rho_f \frac{k}{\eta} (\nabla P + \rho_f g \nabla z) - \rho_f \varepsilon \frac{k}{\eta} \nabla \Pi + \frac{k \Delta H}{\eta T} \nabla T \right) = 0 \quad \text{Eq. 11}$$

with, from left to right in the left-hand-side term, the contribution of the Darcy's flow, the chemical osmosis flow and the thermo-osmosis flow.

### 3.2 Gradients

Figure 3 presents the hydraulic head, concentration and temperature conditions used for the calculations. It includes: i) the heads measured in aquifers surrounding the clayrock [2], ii) the concentration profile of the clayrock porewater expressed in molal unit and calculated by geochemical modeling [23], iii) the temperature profile established at the Tournemire URL and obtained by direct measurement of temperature across the clayrock [24]. The occurrence of a 5 Mavolcanic dyke at a distance of about 2 km from the Tournemire URL likely explains the surprisingly high gradient, almost twice the normal geothermal gradient.



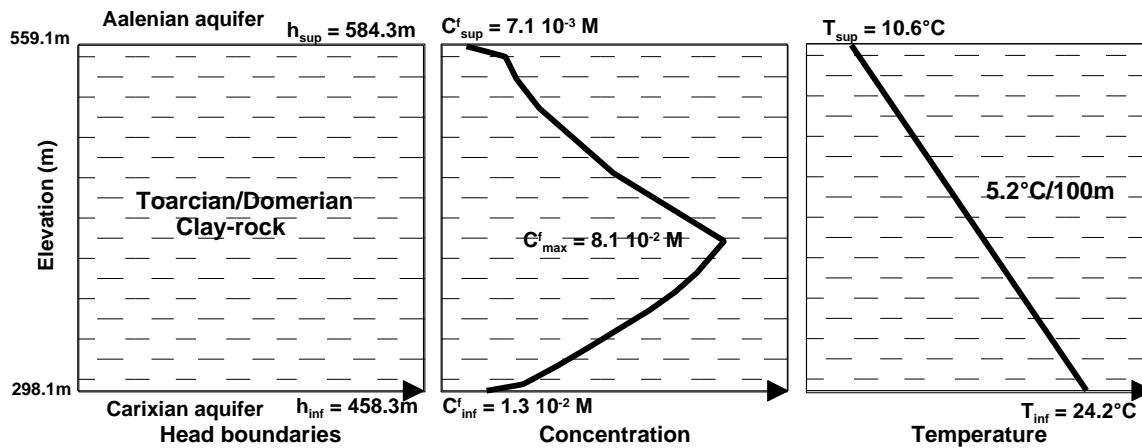


Figure 3: Hydraulic head boundary conditions with temperature and salinity profiles used for calculating the head profile in Tournemireclayrock.

### 3.3 Coupled flow parameters

Additional parameters are needed in the calculations (Eq.11): the dynamic viscosity of water ( $\eta$ ), the fluid density( $\rho_f$ ), the intrinsic permeability ( $k$ ), the chemo-osmotic efficiency $\varepsilon$ , the thermo-osmotic permeability ( $k_T$ ). Their variations across the formation are thus required.

The dynamic viscosity of water ( $\eta$  in Pa s) was calculated from Eq. 6 across the formation and displays values ranging between  $8.95 \times 10^{-4}$  Pa s and  $1.27 \times 10^{-4}$  Pa s, for the highest and the lowest temperature, respectively. The fluid density was determined from the Unesco equation of state [14] and provided computed fluid density in between 998.5 and 1002.3 kg m<sup>-3</sup>, with the highest values linked to the most saline porewaters in the centre of the clayrock formation. The intrinsic permeability profile was calculated from Eq. 4 using petrophysical results obtained across the whole clayrock [25]. The cementation factor  $m$  was fitted to a value of 2.3 for natural clayrock permeabilities and diffusion coefficients [3]. The calculated values range between  $10^{-21}$  and  $10^{-20}$  m<sup>2</sup> (Figure 4) and are of the same order of magnitude as values deduced from pulse tests performed in equipped boreholes [3].

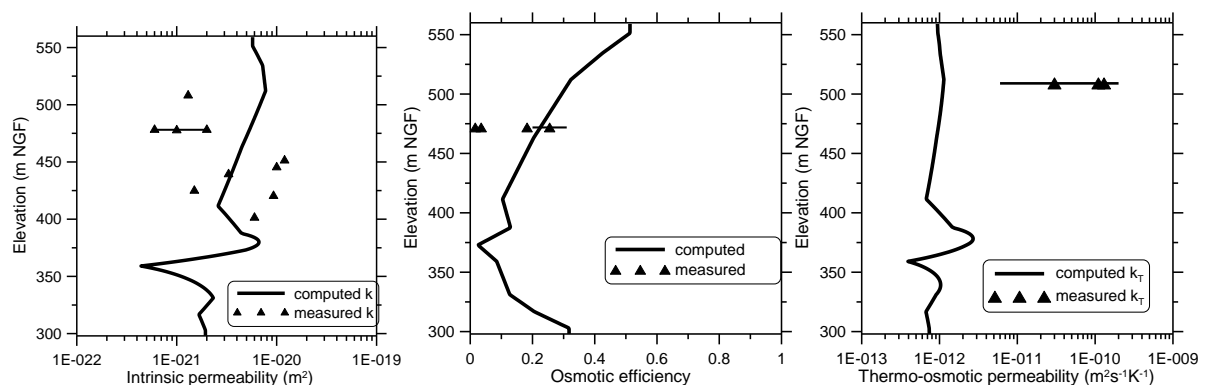


Figure 4: Profiles of measured and computed intrinsic permeability ( $k$ ), chemical osmosis efficiency ( $\varepsilon$ ) and thermo-osmotic permeability ( $k_T$ ) compared to the measured values.

The predicted chemical osmosis efficiency profile across the clayrock (Figure 4) was obtained either by the Bolt expression (Eq. 9 after [11]) in agreement with rock properties and solution composition or through the triple-layer electrical model (TLM) describing the interactions between the charged solid surface of a clayrock and the porewater and taking into account the interactions of adjacent diffuse layers and both monovalent and divalent counter-ions [20]. This profile is compared to values obtained on a clayrock sample. The experiments consisted in inducing a fluid flow through the sample upon a salinity gradient [3]. Efficiency values ranging between 0.014 and 0.31 as a function of the salinity were obtained during these experiments and are in the range of the predicted osmotic efficiencies.



As for the chemical osmotic efficiency, the thermo-osmotic permeability of the Tournemire clayrock was obtained by both predictive calculations and experimental measurements. Predictions of the thermo-osmotic permeability were obtained by a model calculating the excess specific enthalpy in the pore space responsible of the occurrence of thermo-osmosis by molecular interaction considerations [3], [22]. Model input are a set of petrophysical parameters (porosity, specific surface area and cation exchange capacity) and the salinity of the bulk porewater. Taking into consideration the variations of these parameters across the Toarcian/Domerian argillaceous formation, a profile of  $k_T$  is proposed (Fig. 4). The thermo-osmotic permeability of the Tournemire clayrock was also measured during in situ experiments, in an equipped borehole by inducing a temperature gradient between test section of the borehole and the clayrock [24]. A temperature gradient was induced. The inversion of the pressure evolution in the chamber allowed identifying a range of thermo-osmotic permeabilities with  $k_T$  values ranging between  $6 \cdot 10^{-12}$  and  $2 \cdot 10^{-10} \text{ m}^2 \text{ s}^{-1} \text{ K}^{-1}$  (Figure 4). In this figure, the measured thermo-osmotic permeabilities are one order of magnitude greater than the predicted one, likely underestimated.

### 3.4 Contribution of flows to head profile

The contribution of each individual transport phenomena to the fluid pressure is evaluated by solving the pressure - diffusion equation at steady-state (Eq.11). Results are reported in Figure 5.

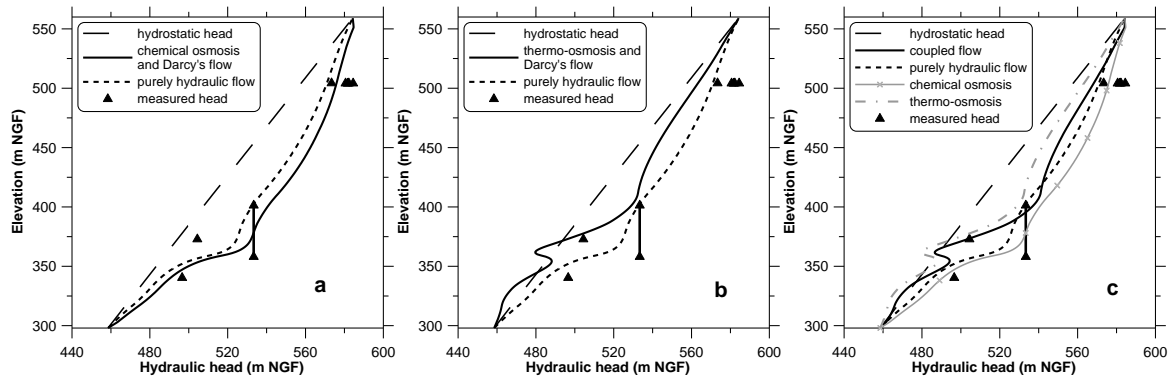


Figure 5: Contribution of the chemical-osmosis (a) and thermo-osmosis (b), and fully-coupled flows (c) to the head profile compared to a pure hydraulic flow.

#### 3.4.1 Darcy flow

For a pure hydraulic flow eq.11 becomes:

$$\frac{\partial}{\partial z} \left( \rho_f \frac{k}{\eta} (\nabla P + \rho_f g \nabla z) \right) = 0 \quad \text{Eq. 12}$$

And  $\sigma$ , the deviation between the measured and calculated head, is estimated from:

$$\sigma = \frac{|\Delta h_{data} - \Delta h_{model}|}{\Delta h_{data}} \times 1000 \quad \text{Eq. 13}$$

Eq.12 gives a linear hydraulic head profile when the hydraulic parameters are taken constant across the clayrock ( $k = 10^{-21} \text{ m}^2$ ,  $\eta = 10^{-3} \text{ Pa s}$ ,  $\rho_f = 10^3 \text{ kg m}^{-3}$ ), thus providing access to the hydrostatic head profile. The computed head profile displays spatial variations with a deviation of 24 % compared to the measured heads when hydraulic parameters are allowed to vary (Figure 4). The effect of the intrinsic permeability is the most significant on the head profile, although the variations of the fluid viscosity are also non-negligible. The specific discharge  $q$  is  $-1.3 \cdot 10^{-14} \text{ m s}^{-1}$ , the negative value indicating a water movement directed downward.

### 3.4.2 Chemical osmosis

The head profile across the formation induced by chemical osmosis is calculated from (Eq. 11) which is restricted to Darcy's flow and chemical osmosis so that the solved equation becomes:

$$\frac{\partial}{\partial z} \left( \rho_f \frac{k}{\eta} (\nabla P + \rho_f g \nabla z) - \rho_f \varepsilon \frac{k}{\eta} \nabla \Pi \right) = 0 \quad \text{Eq. 14}$$

Addition of chemical osmosis to the Darcy's flow leads to increase of 8 m the excess-heads at the centre of the clayrock (Figure 5a) compared to those obtained with Darcy's flow alone. The calculated hydraulic head profile is close to the measured one, so that a deviation of 16 % is found between the model and the measured data, thus chemical osmosis does not induce significant changes on the head profile which is likely due to the weak porewater concentration profile across the Toarcian/Domerian clayrock. The specific discharge is of  $1.4 \cdot 10^{-14} \text{ m s}^{-1}$  with a water movement still directed downward.

### 3.4.3 Thermo-osmosis

Considering only thermo-osmosis and Darcy's flows, Eq. 11 becomes:

$$\frac{\partial}{\partial z} \left( \rho_f \frac{k}{\eta} (\nabla P + \rho_f g \nabla z) + \frac{k \Delta H}{\eta T} \nabla T \right) = 0 \quad \text{Eq. 15}$$

The introduction of thermo-osmosis, together with the Darcy's flow, leads to a hydraulic head lower than the one calculated with a purely hydraulic flow (Figure 5b). The resulting head profile is between 10 and 15 m less for the upper Toarcian and up to 35 m less in the lower Toarcian. In the deepest part of the formation, the head is even slightly lower than the hydrostatic head. It results in a higher deviation (84 %). The specific discharge is of  $3.3 \cdot 10^{-14} \text{ m s}^{-1}$  and its positive value indicates an upward water movement attributed to the thermo-osmotic flow.

### 3.4.4 All coupled flows

Coupling all flows by applying Eq. 11 provides a maximum excess head of 25 m at the clayrock centre and an excess-head almost nil below (Figure 5c). A deviation of 59 % to the measured hydraulic head profile is found. The influence of the thermo-osmosis on the trend of the calculated hydraulic head with coupled flows is obvious. When both chemo- and thermo-osmosis and Darcy's flow are considered, a specific discharge of  $3.2 \cdot 10^{-14} \text{ m s}^{-1}$  is computed, close to the one calculated for thermo-osmosis and Darcy's flow, and indicates an upward water movement.

Steady-state conditions were postulated in Eq. 11 because of uncertainties on the conditions that constrain the calculations of evolution of the flows and transfers at geological time-scales. Nevertheless, because of the transient conditions of the concentration profile, two simple calculations at transient-state were performed. One of these calculations considers chemical osmosis and Darcy's flow and the second one gathers chemical osmosis, thermo-osmosis and Darcy's flow. The diffusion scenario for the Tournemire argillaceous formation [25],[26] was reproduced in these calculations and a Fick's diffusion was involved from a seawater salinity to a salinity profile close of the present-day profile using a diffusion coefficient in the range of those measured at Tournemire.

At final transient-state, the hydraulic head profiles and specific discharges are very close to those calculated assuming a quasi-steady-state. This observation allows asserting that the hypothesis of a pseudo-equilibrium of fluid flow for a given concentration profile is valid. The steady-state conditions can then be assumed with confidence and the calculations results are very likely realistic.

### 3.5 Contribution of coupled flows to mass transport of RN

The modification of the fluid movement caused by osmotic processes was shown to turn upward when thermo-osmosis is introduced in the calculations. The real interest of the fluid flow direction lies in its potential impact on advection mass transport. For this purpose, the Peclet number was calculated for estimating the advection vs. diffusion contribution to the mass transport. The Peclet number,  $Pe$ , can be established as the ratio of the characteristic times for diffusion  $\tau_D = \frac{L^2}{D_p}$  to advection  $\tau_a = \frac{L}{u}$ , where  $L$  is the thickness (m) of the porous medium crossed by the solute,  $D_p = \frac{D_e}{\omega_{anions}}$ ,  $D_p$  and  $D_e$  stand for the pore and effective diffusion coefficients, respectively ( $\text{m}^2 \text{s}^{-1}$ ) and  $\omega_{anions}$  is the anions accessible porosity.  $u$  is the pore fluid velocity ( $\text{m s}^{-1}$ ) related to the specific discharge  $q$  by the relation  $u = q/\omega_k$ , where  $\omega_k$  is the kinematic porosity or porosity accessible to flow. The Peclet number thus writes:  $Pe = Lq/D_p\omega_k$ .

The Peclet numbers for the Tournemire argillaceous formation were determined for  $\text{Cl}^-$ , as  $^{36}\text{Cl}$  is one of the most mobile radionuclide, at the center of the 250 m thick formation ( $L = 125$  m), using an effective diffusion coefficient for  $\text{Cl}^-$  of  $4 \cdot 10^{-12} \text{ m}^2 \text{s}^{-1}$  [25] and the specific discharges reported previously.

The kinematic porosity value ranges between the total porosity and the accessible porosity which are 8.8 % and 6.6 % for  $\text{Cl}^-$ , respectively [25]. Calculation uses the total porosity as kinematic porosity. The resulting Peclet number is 0.28 for the purely hydraulic flow, 0.30 for chemical osmotic and Darcy's flows, 0.71 for the thermo-osmotic and Darcy's flows and 0.69 for all coupled flows. These calculated Peclet numbers slightly lower than 1 suggest that diffusion is dominant but the advective flow is not negligible for mass transport at the formation scale. Advection has also to be taken into consideration for mass transport especially if thermo-osmosis is considered, because of the underestimation of the modeled thermo-osmotic permeability compared to the measured values. This is in contradiction with the general assumption that solute transport in a compacted clayrock is mainly controlled by diffusion.

### 3.6 Contribution of hydromechanical processes to head profile

#### 3.6.1 Viscoplastic behaviour of clays

The visco-plastic behavior of clayrocks results in a delayed deformation. Here, our interest to the visco-plastic behaviour of clays is limited to the time dependent volumetric deformation (one rock deformation mechanism) and can lead to a persistence of overpressures during large geological time scales. The macroscopic volumetric creep of the rock, or compaction creep, can result from granular mechanisms like pressure dissolution, in carbonates and sandstones, or sliding and rotation of grains and platelets leading to an aggregate deformation, in clays.

A calculation of the excess pressure caused by the visco-plastic behavior of the Tournemire clayrock was made to assess the possible contribution of creep to the present measured pressure profile. This calculation was made for a 1D geometry, along the  $z$  axis and the equation to be solved is:

$$K \frac{\partial P}{\partial z} = S_s \frac{\partial P}{\partial t} - \rho_f \frac{\sigma}{\eta_s(t)} \quad \text{Eq. 16}$$

Where  $K$  is the hydraulic conductivity ( $\text{m s}^{-1}$ ),  $S_s$  is the specific storativity ( $\text{m}^{-1}$ ),  $\sigma$  the total stress (Pa), and  $\eta_s(t)$  is the volumetric viscosity coefficient of the porous medium (Pa s).

A relation describing the viscosity coefficient evolution with time was obtained from an inversion of the volumetric deformation measured on the Toarcian clay [27] and writes:

$$\eta_s(t) = 3.5 \cdot 10^{11} \times t^{0.9} \quad \text{Eq. 17}$$

This time dependent relationship gives a  $\eta_s(t)$  value of  $6 \cdot 10^{23}$  Pa s after 1 Ma of creep.

The main uncertainty in the calculation input lies in fixing time since the present total stress conditions are established. A calculation was performed assuming that the present-day total stress of  $4 \pm 1$  MPa has not changed since 34 Ma which corresponds to the end of the Pyrenean orogeny, the last noticeable tectonic event [28]. Two other times were tested as they likely have modified the total stress: 5 Ma ago, at the end of the valley incision, and at 2 Ma, the start of the glacial period.

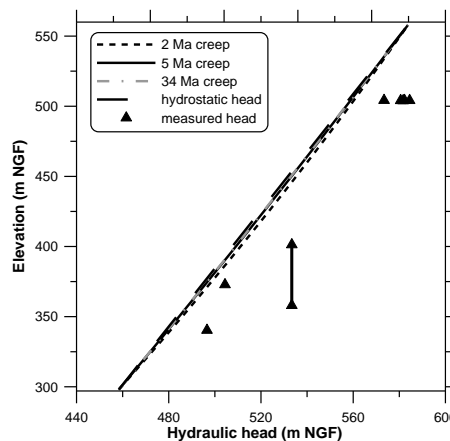


Figure 6: Calculated contribution of creep on the hydraulic head profile in Tournemire clayrock.

Calculations were made for constant  $K = 10^{-14} \text{ m s}^{-1}$ ,  $S_s = 10^{-6} \text{ m}^{-1}$ ,  $\sigma = 4$  MPa and the time-dependent variable  $\eta_s(t)$  from eq. 17. The results shown in Figure 6 indicate a very limited influence of this phenomenon on the pressure profile. The excess head, related to the hydrostatic head, is of few meters and tends to decrease with time without completely vanishing. Indeed, after 2 Ma of viscous behavior an excess head around 3.7 m is calculated while after 5 Ma the excess head is around 1.6 m and around 1.3 m after 34 Ma.

### 3.6.2 Other possible processes

Other possible causes for an excess-head are erosion unloading, lateral tectonic compression and compaction disequilibrium. All these processes are unlikely due i) to the exceptional over-consolidated nature of the clayrock acquired a very long time ago since the Cretaceous times when more than 1000 meters of sediments were eroded, ii) the long delay since the last tectonic event (about 34 Ma).

## 4 CONCLUSIONS

In very impervious clayrocks, like the Callovo-Oxfordian (COx) studied by Andra as a potential host rock for the disposal of HL-ILLL radioactive wastes, pore pressure, and their related hydraulic heads, frequently show excess-heads with respect to the theoretical hydrostatic head profile driven by the surrounding aquifers. The origin of such excess head was still a subject of controversy since it may result from many processes including transport and hydromechanical processes. An overpressure of 30m is being measured in the Toarcian/Domerian clayrock at Tournemire URL whereas it is of about 50m for the COx centre at the Bure URL.

This paper aimed at identifying and quantifying the contribution of each cause to the excess-head measured at Tournemire and their possible contribution to the transport of radionuclides. A special focus was made on transport processes and especially on advection, the diagonal transport process, and on chemo-osmosis and thermo-osmosis, the non-diagonal one, respectively responsible for a fluid flow under gradients of pressure, concentration and temperature.

Osmotic processes are expected to develop due to the small pore size and the electrostatic interactions related to the charged surface of clay minerals. The quantification of their relative contribution has required the acquisition of their force gradients and of their related parameters hereinafter referred permeabilities. The force gradients for P,T,C were obtained by direct measurements (P,T) at Tournemire and indirectly by geochemical modeling (C). Darcy permeability was deduced from petrophysical measurements. Chemo-osmotic and thermo-osmotic permeabilities were obtained from on-site and lab experiments and by theoretical models with petrophysical parameters and medium conditions (porewater composition and temperature) as input parameters.

A 1D modeling approach based on the application of continuity equation at steady state was proposed to assess the individual or coupled contribution of flow transport processes. A satisfactory reproduction of the measured excess-hydraulic head was achieved by coupling chemical osmosis, thermo-osmosis and advection which alone are able to generate, in the present-day conditions, an excess-head in Tournemire clay rock.

The contribution of hydromechanical processes (e.g., the visco-plastic behaviour of clays, erosion unloading, lateral tectonic compression and compaction disequilibrium) was also assessed but their contribution to the measured excess-head looks very unlikely. To conclude, only the transport processes, related to the intrinsic permeability variation across the formation coupled to non-diagonal osmotic processes can explain the pressure field in the Toarcian/Domerian formation at the Tournemire URL. Those calculations also allowed a comparison of the characteristic times for diffusion and advection. Results suggest that diffusion still remains the dominant transport phenomenon for solutes and therefore for RN at the formation scale, so far, but the contribution of advection cannot be neglected as the Peclet number is 0.7, not that far from 1. This indicates that the coupled fluid flows also have to be taken into account for mass transport. This is especially true if thermo-osmosis is considered because of the underestimation of the modeled thermo-osmotic permeability compared to the measured values and also because its introduction in the calculations leads to an increase of the specific discharge and to inverse the water movements which become directed upward.

## 5 REFERENCES

- [1] Andra (2005) – Dossier argile 2005 - <http://www.andra.fr/download/site-principal/document/editions/269.pdf>
- [2] Matray, J.-M., Savoye, S., and Cabrera, J. (2007) Desaturation and structure relationships around drifts excavated in the well-compacted Tournemire's argillite (Aveyron, France). *Engineering Geology* 9, p1-16.
- [3] Tremosa, J. (2010), Influence of osmotic processes on the excess-hydraulic head measured in the Toarcian/Domerian argillaceous formation of Tournemire, Ph.D. thesis, Université Pierre et Marie Curie, Paris 6, France.
- [4] Gonçalves J., Violette, S., Wendling, J. (2004) Analytical and numerical solutions for alternative overpressuring processes: application to the Callovo-Oxfordian sedimentary sequence in the Paris basin, France. *J. Geophys. Res.* 109, B02110.1–B02110.14.

- [5] Neuzil, C. E. (1995), Abnormal Pressures as Hydrodynamic Phenomena, American Journal of Science, 295, 742-786.
- [6] IRSN (2005) – Avis de l'IRSN sur le Dossier 2005 Argile - [http://www.irsn.fr/FR/expertise/rapports\\_expertise/Documents/surete/IRSN\\_rapport\\_2005\\_argile.pdf](http://www.irsn.fr/FR/expertise/rapports_expertise/Documents/surete/IRSN_rapport_2005_argile.pdf).
- [7] Rousseau-Gueutin, P. (2008) Les processus couplés dans les argilites du Callovo-Oxfordien sur le site de Bure : implications pour les mouvements de fluide et de solutés. PhD thesis, Université Pierre et Marie Curie, Paris VI, 2008.
- [8] Mitchell, J. K., and K. Soga (2005) Fundamentals of Soil Behavior, 3rd ed., 558 pp., John Wiley, N. Y.
- [9] Onsager, L. (1931a) Reciprocal relations in irreversible processes. I. Phys. Rev. 37, 405.
- [10] Onsager, L. (1931b) Reciprocal relations in irreversible processes. II. Phys. Rev. 38, 2265.
- [11] Bolt, G. H. (1979) Soil Chemistry, B. Physicochemical Models, 480 pp., Elsevier, Amsterdam, Netherlands.
- [12] A. Katchalsky, P.F. Curran, Nonequilibrium Thermodynamics in Biophysics, Harvard University Press, Cambridge, Massachusetts, 1967.
- [13] Revil and Leroy, 2004 Revil, A., and P. Leroy (2004), Constitutive equations for ionic transport in porous shales, J. Geophys. Res., 109, B03208, doi:10.1029/2003 JB002755.
- [14] Unesco (1980) Tenth report on the joint panel on oceanographic tables and standard. Sidney, BC, Canada. 1-5 september 1980. Unesco technical paper in marine science 36, 1981. <http://unesdoc.unesco.org/images/0004/000461/046148eb.pdf>
- [15] Mercer, J. W., Pinder, G. F., and Donalson, I. G. A (1975) Galerkin-finite element analysis of the hydrothermal system at Wairakei, New-Zealand. Journal of Geophysical Research 80, 2608-2621.
- [16] Bresler, E. (1973) Anion exclusion and coupling effects in nonsteady transport unsaturated soils: I. Theory, Soil Sci. Soc. Am. Proc., 37(5), 663–669.
- [17] Fritz, S. J. (1986) Ideality of clay membranes in osmotic processes: A review, Clays Clay Miner., 34(2), 214–223.
- [18] Gonçalves, J., P. Rousseau-Gueutin, and A. Revil (2007) Introducing interacting diffuse layers in TLM calculations. A reappraisal of the influence of the pore size on the swelling pressure and the osmotic efficiency of compacted bentonites, J. Colloid Interface Sci., 316, 92–99.
- [19] Neuzil, C. E., and A. M. Provost (2009) Recent experimental data may point to a greater role for osmotic pressures in the subsurface, Water Resources Research, 45, W03410, doi:10.1029/2007WR006450.
- [20] Tremosa, J., Gonçalves, J., Matray, J.M. (2012) Natural conditions for more limited osmotic abnormal fluid pressures in sedimentary basins. Water Resources Research, Vol. 48, W04530, doi:10.1029/2011WR010914.
- [21] Gonçalves, J., Tremosa, J. (2010). Thermo-osmosis in clayrocks: I theoretical insights. J. Colloid Interface Sci. 342, 166–174.
- [22] Gonçalves, J., de Marsily G., Tremosa, J. (2012) Importance of thermo-osmosis for fluid flow and transport in clay formations hosting a nuclear waste repository Earth and Planetary Science Letters 339–340 1–10, <http://dx.doi.org/10.1016/j.epsl.2012.03.032>



- [23] Tremosa, J., Arcos D., Matray J.M., Bensenouci F., Gaucher E.C., Tournassat C., Hadi J. (2012) Geochemical characterization and modelling of the Toarcian/Domerian porewater at the Tournemire underground research laboratory. *Applied Geochemistry* 27 1417–1431 doi:10.1016/j.apgeochem.2012.01.005
- [24] Tremosa, J., Gonçalves, J., Matray, J.M., Violette, S. (2010) Thermo-osmosis in clay-rocks: II in-situ experimental approach. *J. Colloid Interface Sci.* 342, 175–184.
- [25] Bensenouci, F. (2010) Apport des traceurs naturels à la compréhension des transferts au sein des formations argileuses compactées. Ph.D. thesis. Univ. Paris-Sud 11.
- [26] Savoye, S., Michelot, J. L., Bensenouci, F., Matray, J. M., and Cabrera, J. (2008) Insight given by stable isotope profiles in pore-water for understanding transfers through Toarcian/Domerian argillaceous rocks over large space and time scales. *Physics and Chemistry of the Earth* 33, S67-S74.
- [27] Fabre, G., and Pellet, F. (2006) Creep and time-dependent damage in argillaceous rocks. *International Journal of Rock Mechanics and Mining Science* 43, 950-960.
- [28] Cabrera, J., Beaucaire, C., Bruno, G., De Windt, L., Genty, A., Ramambasoa, N., Rejeb, A., Savoye, S., and Volant, P. (2001) *Projet Tournemire. Synthèse des programmes de recherche.* Rapport DPRE/SERGD 01-19, IRSN.